





# Mucosal adhesion phenomenon after maxillary sinus floor elevation: A preclinical study

Yasushi Nakajima<sup>1,2</sup> | Karol Alí Apaza Alccayhuaman<sup>2,3</sup>  | Daniele Botticelli<sup>2</sup>  |  
Niklaus Peter Lang<sup>4</sup>  | Ermenegildo Federico De Rossi<sup>2</sup> | Samuel Porfirio Xavier<sup>2,5</sup> 

<sup>1</sup>Department of Oral Implantology, Osaka Dental University, Osaka, Japan

<sup>2</sup>ARDEC Academy, Rimini, Italy

<sup>3</sup>Department of Oral Biology, Medical University of Vienna, Vienna, Austria

<sup>4</sup>School of Dental Medicine, University of Bern, Bern, Switzerland

<sup>5</sup>Department of Oral and Maxillofacial Surgery and Periodontology, Faculty of Dentistry of Ribeirão Preto, University of São Paulo, São Paulo, Brazil

## Correspondence

Karol Alí Apaza Alccayhuaman, Department of Oral Biology, Medical University of Vienna, Vienna, Austria.

Email: [caroline7\\_k@hotmail.com](mailto:caroline7_k@hotmail.com)

Daniele Botticelli, ARDEC Academy, viale Giovanni Pascoli 67, Rimini, Italy.

Email: [daniele.botticelli@gmail.com](mailto:daniele.botticelli@gmail.com)

## Funding information

ARDEC Academy

## Abstract

**Aim:** To describe the histological events that occur after maxillary sinus floor elevation when the elevated and undetached sinus mucosa are in close proximity or in contact with each other.

**Materials and methods:** From 76 rabbits, 152 elevated maxillary sinuses were analyzed histologically. Sites without adhesions were classified as “No proximity,” whereas the adhesion stages were divided into “Proximity,” “Fusion,” and “Synechia stages.” The width of the pseudostratified columnar epithelium and the distance between the two layers of the elevated and undetached sinus mucosae were measured at various standardized positions.

**Results:** Thirty-one sites presenting with adhesions were found. Twelve sites were in the proximity stage,” presenting cilia of the two epithelial layers that were shortened and interlinked within the mucous context. Hyperactivity of the goblet cells was also observed. In the other cases, the hyperplastic epithelium showed attempts to reach the contralateral mucosa. The 15 “fusion stage” sites presented regions with epithelial cells of the two mucosal layers that penetrated each other. Four sites presented “synechia stages,” represented by bridges of connective tissue connecting the two lamina propria.

**Conclusions:** Close proximity or tight contact between the elevated and undetached mucosa adhering to the bone walls might occur after maxillary sinus floor elevation. This induced hyperplasia of the epithelial cells and adhesion of the two layers until synechia formation.

## KEYWORDS

biomaterial, bone healing, maxillary sinus elevation, Schneiderian membrane, synechia

## 1 | INTRODUCTION

The edentulous alveolar bony crest can be restored using fixed dental prostheses anchored on osseointegrated implants. However, when the bone volume in the posterior segments of the maxilla is insufficient for implant installation, sinus floor elevation may have to be

performed. Several techniques have been proposed to increase the maxillary bone volume and resulted in optimal clinical outcomes (Del Fabbro et al., 2013; Pjetursson et al., 2008; Tan et al., 2008). Before performing this technique, an accurate analysis of the anatomical conditions must be performed (Kawakami, Botticelli, Nakajima, Sakuma & Baba, 2019). After sinus floor elevation, the elevated

This is an open access article under the terms of the [Creative Commons Attribution-NonCommercial-NoDerivs](https://creativecommons.org/licenses/by-nc-nd/4.0/) License, which permits use and distribution in any medium, provided the original work is properly cited, the use is non-commercial and no modifications or adaptations are made.

© 2023 The Authors. *Clinical Oral Implants Research* published by John Wiley & Sons Ltd.

space generally acquires a convex dome shape as documented by tomographic studies (Kawakami et al., 2018; Kawakami, Lang, Ferri, Apaza Alccayhuaman & Botticelli, 2019). This convex shape may be maintained over time if biomaterials with a low resorption rate are used (Figure 1a–d). The undetached mucosa at the sinus bony walls (U-SM) provides a region [mucosal folding region (MFR)] from which the elevated sinus mucosa (E-SM) is lifted cranially (Figure 1a,b). The elevated mucosa approaches the undetached mucosa lining the bony walls and, in some cases, may come into close proximity or in contact with each other (Figure 1a–d). In the first healing period, such conditions may be favored by postsurgical edema (Guo et al., 2016; Makary et al., 2016; Figure 1a,b), which may involve the ostium and infundibulum of the sinus (Sakuma et al., 2020). Moreover, the mucociliary function of the sinus may be also affected (Griffa et al., 2010; Torretta et al., 2012). However, the fate of the two mucosae in contact remains unknown. Therefore, the aim of the present study was to describe the histological events that occur after maxillary sinus floor elevation when elevated and undetached sinus mucosae come into close proximity or are in contact with each other.

## 2 | MATERIALS AND METHODS

### 2.1 | Ethical statements

The main outcomes of healing within the subantral elevated space after sinus floor elevation in rabbits have been reported previously (Ferreira Balan et al., 2022; Godoy et al., 2021; Hirota et al., 2020; Masuda et al., 2020). All experiments were approved by the Ethical Committee of the Faculty of Dentistry of Ribeirão Preto, University of São Paulo: experiment (Ferreira Balan et al., 2022) approved on April 8, 2019, protocol No. 2019.1.113.58.1; experiments (Godoy et al., 2021; Masuda et al., 2020) approved on June 14, 2017, protocol 2017.1.278.58.9; and experiment (Hirota et al., 2020), approved on March 21, 2018, protocol 2018.1.10.58.7. Brazilian rules for animal care were strictly followed. The same histological material was further analyzed, and the present study reports data on sinus mucosal healing after sinus floor elevation. This study followed the ARRIVE guidelines.

### 2.2 | Experimental animals

A total of 152 elevated sinuses in 76 New Zealand white rabbits, weighing approximately 3.5–4.0 kg and 5–6 months of age, were analyzed.

### 2.3 | Study design and biomaterials used

All four experiments included the simulation of a bilateral sinus floor elevation procedure in a rabbit model.

In experiment E1 (Ferreira Balan et al., 2022), xenograft granules of either Bio-oss® 0.250–1.0 mm or Cerabone® 0.5–1 mm were

randomly grafted within elevated spaces in 20 rabbits. Healing was evaluated after 2 and 10 weeks ( $n = 10$  for each period).

In experiment E2 (Godoy et al., 2021), xenograft granules of different sizes (Bio-oss® 0.250–1.0 or 1–2 mm) were randomly grafted within elevated spaces in 18 rabbits. Healing was evaluated after 2, 4, and 8 weeks ( $n = 6$  for each period).

In experiment E3 (Hirota et al., 2020), xenograft granules (Bio-oss® 0.250–1.0 mm) were used bilaterally in 20 rabbits. At randomly selected test sites, the granules underwent argon plasma treatment before being grafted within the elevated space. The granules on the control side did not receive plasma treatment. Healing was evaluated after 2 and 10 weeks ( $n = 10$  for each period).

In experiment E4 (Masuda et al., 2020), xenograft granules of different sizes (Bio-oss® 0.250–1.0 or 1–2 mm) were randomly grafted within the elevated spaces in 18 rabbits, and implants were installed simultaneously and bilaterally. Healing was evaluated after 2, 4, and 8 weeks ( $n = 6$  for each period).

### 2.4 | Biomaterial characteristics

Bio-Oss® (Geistlich Biomaterial) is a deproteinized bovine bone mineral with sinterization at 300°C, porosity of 75%–80%, pores of 20–200 µm, and a particulate size of 0.5–1 mm (Figueiredo et al., 2010).

Cerabone® (Botiss Biomaterials GmbH) is composed of hydroxyapatite from bovine cancellous bone, with sintering at 1200°C, porosity of 65%–80%, with pores of 600–900 µm, and an average particle size of 0.5–1 mm (Figueiredo et al., 2010).

Bio-Gide is a bilayer collagen membrane composed of porcine collagen (Geistlich Biomaterial).

### 2.5 | Randomization and allocation concealment

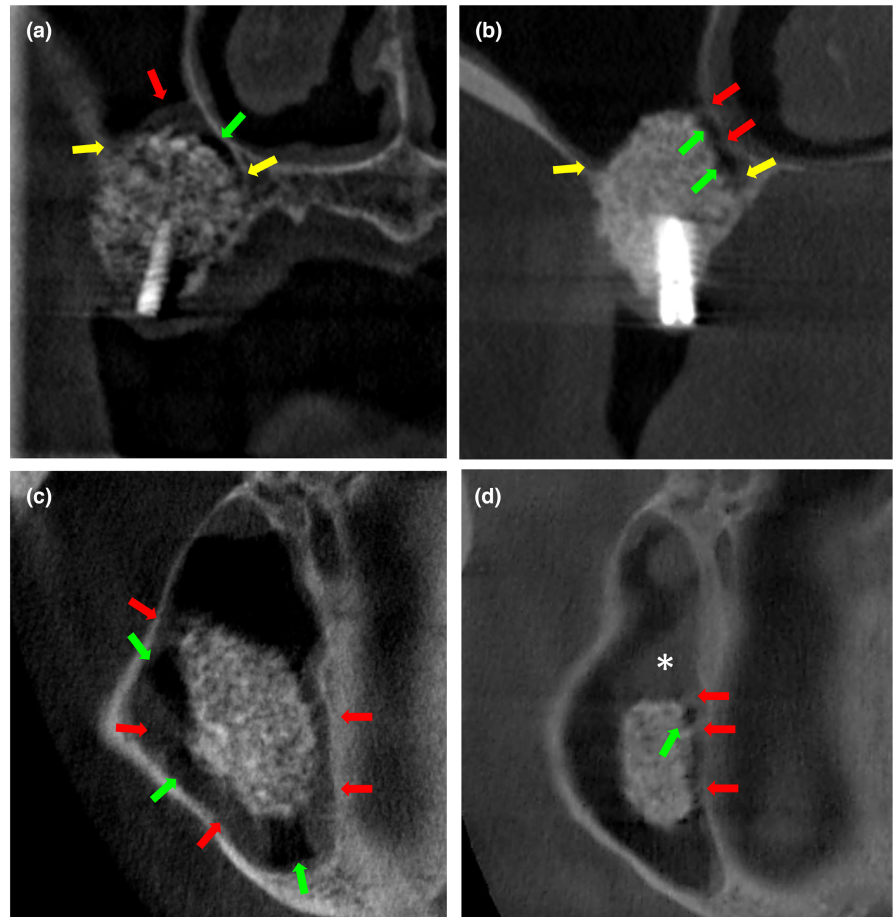
Each experiment adhered to strict randomization protocols and allocation concealment. Readers are advised to consult the original publications for further information.

### 2.6 | Surgical procedures

The anesthetic procedures were similar in all four experiments and performed with injection of 1.0 mg/kg acepromazine (1Acepran®), 3.0 mg/kg xylazine (Dopier®, Hertape Calier), and 50 mg/kg ketamine hydrochloride (Etamin Agener, União Química Pharmaceutical Nacional S/A).

Skilled maxillofacial surgeons performed all the surgeries. An incision was made on the nasal dorsum and the nasal bone was exposed. One osteotomy was performed bilaterally to the nasoincisor suture. The subantral spaces obtained after sinus mucosa elevation were filled with the grafts. Implants were placed in one of the experiments (Masuda et al., 2020), whereas collagen membranes (Bio-Gide® Geistlich Biomaterials) were used to cover the osteotomies in other experiments (Ferreira Balan et al., 2022; Godoy et al., 2021;

**FIGURE 1** Cone-beam computed tomographs showing adhesion sites after 9 months of healing. (a, b) Coronal view; (c, d) axial view. Note enclosed regions (green arrows), probably tubular in shape, delimited by adhesion structures (red arrows). Yellow arrows, mucosa folding regions (MFR); \*Sinus mucosa distal to the elevated region.



Hirota et al., 2020). The wounds were then closed using single sutures in two planes.

## 2.7 | Maintenance

The animals were housed in individual cages in a climate-controlled room. Food and water were provided ad libitum. Professionals monitored biological functions and wounds. Antibiotics and analgesics were administered postsurgically.

## 2.8 | Euthanasia

The rabbits were first anesthetized following similar procedures described above and then euthanized either with an overdose of sodium thiopental (1.0g, 2mL; Thiopental®, Cristália Produtos Químicos Pharmaceutics; Godoy et al., 2021; Hirota et al., 2020; Masuda et al., 2020) or in a closed transparent acrylic box containing gas carbon dioxide (CO<sub>2</sub>) (Ferreira Balan et al., 2022).

## 2.9 | Histological preparation

The biopsies were retrieved in blocks by an expert from the histology lab, fixed in 10% formaldehyde, dehydrated, embedded in resin (LR White Hard Grid, London Resin Co. Ltd), and polymerized. The

biopsies were then processed using precision cutting and grinding equipment (Exakt® Apparatebau). Two histological slides from each biopsy were obtained and stained with either toluidine blue or Stevenel's blue and alizarin red.

## 2.10 | Histometric evaluations

Evaluations were performed around the region where the sinus mucosa was elevated (mucosa folding region; MFR), both at the medial and lateral aspects (Figure 2a). This region was delimited by the elevated sinus mucosa (E-SM) opposite to the undetached sinus mucosa (U-SM) lining the sinus bony walls.

Four stages were defined based on the interactions observed between the elevated and undetached sinus mucosae.

1. "No proximity," all sites with elevated and undetached sinus mucosae not in close proximity.

### Adhesion phenomena

2. "Proximity," when elevated and undetached sinus mucosae were in contact with each other or in close vicinity with mucous interposed.
3. "Fusion," when the epithelial cells of elevated and undetached sinus mucosae were interpenetrating or fused between each other.

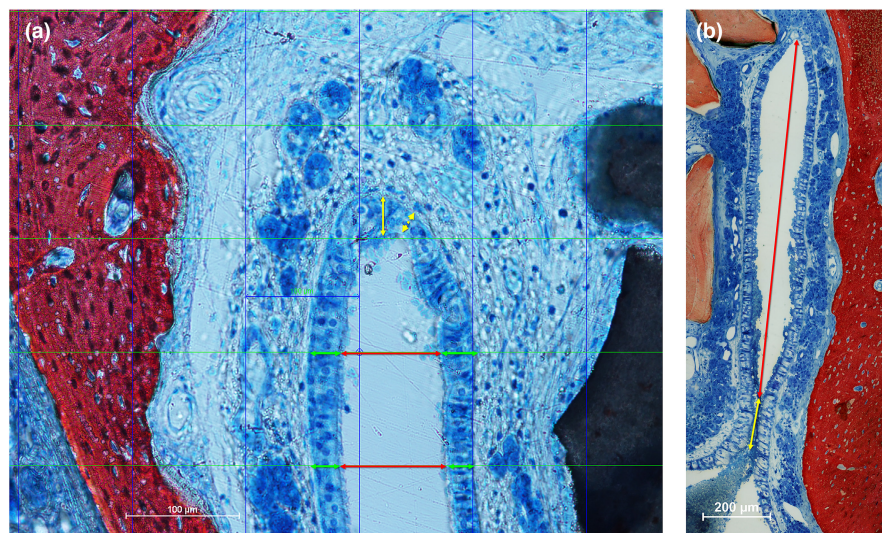


**FIGURE 2** (a) Width of the thinnest epithelial layer within  $\sim 50\mu\text{m}$  from the mucosa folding region evaluated in both U-SM and E-SM (dotted yellow arrow); width of the epithelial layer in the center of the mucosa folding region (yellow arrow) and at  $\sim 100$  and  $\sim 200\mu\text{m}$  in both U-SM and E-SM (green arrows); distance between U-SM and E-SM at  $\sim 100$  and  $\sim 200\mu\text{m}$  from MFR (red arrows). (b) Distance of the adhesion from the MFR (red arrow) and length of adhesion (yellow arrow). The elevated site can be recognized by the presence of biomaterial.

	No. of rabbits	No. of weeks (no. of rabbits)	No. of sinuses	No. of MFR	No. of adhesion sites
E1	20	2 (10); 10 (10)	40	80	9
E2	18	2 (6); 4 (6); 8 (6)	36	72	4
E3	20	2 (10); 10 (10)	40	80	12
E4	18	2 (6); 4 (6); 8 (6)	36	72	6
Total	76		152	304	31

**TABLE 1** Number of rabbits included and periods, sinuses, MFR, and adhesion sites analyzed.

Note: E1, Ferreira Balan et al., 2022; E2, Godoy et al., 2021; E3, Hirota et al., 2020; and E4, Masuda et al., 2020.

Abbreviation: MFR, mucosa folding region.

4. "Synechia," when the lamina propria of both mucosae bridged together.

Moreover, the presence of multiple adhesions and synechia resulting in enclosed regions completely surrounded by epithelium has been reported.

The stages were evaluated at the medial and lateral aspects of both sinuses on one histological slide (Stevenel's blue and alizarin red staining). Seventy-six histological slides representing 152 sinuses were analyzed. However, histological measurements were performed in all sinuses of the experiment (Ferreira Balan et al., 2022) and at sinuses presenting the adhesion phenomenon in the other three experiments (Godoy et al., 2021; Hirota et al., 2020; Masuda et al., 2020).

The following measurements were performed (Figure 2a): width of the thinnest epithelial layer within  $\sim 50\mu\text{m}$  from the mucosa folding region (MFR) evaluated in both U-SM and E-SM; width of the epithelial layer in the center of the MFR and at  $\sim 100$  and  $\sim 200\mu\text{m}$  from the MFR in both U-SM and E-SM; and the distance between U-SM and E-SM at a distance from the MFR of  $\sim 100$  and  $\sim 200\mu\text{m}$ .

In the region with adhesion phenomena, the following measurements were performed (Figure 2b): distance of the adhesion from the MFR, length of adhesion, minimum distance between U-SM and E-SM, maximum width of the epithelial layer, and width of the epithelial layer in the U-SM region located far away from the adhesion phenomenon

( $\sim 500\mu\text{m}$  between the two mucosal layers; pristine sinus mucosa; P-SM). The limits of the adhesions were determined subjectively.

## 2.11 | Data analysis

Histological measurements were performed twice by an assessor (EFDR) and the mean values were obtained. Before undertaking measurements, calibration was performed with another expert examiner (DB).

The primary variable was the height of the epithelial layers. Additional variables were used to describe the adhesion phenomenon.

Prism 9.1.1 (GraphPad Software, LLC) was used for statistical analyses. The normal distribution of the variables was assessed using the Shapiro–Wilk test for both paired and unpaired variables. A paired t-test or Wilcoxon test was used to evaluate the differences between the groups.

The level of significance was set at  $\alpha = 0.05$ .

## 3 | RESULTS

Table 1 specifies the number of animals, sinuses, MFR evaluated, and the number of adhesion phenomena found for each study.

### 3.1 | Descriptive histological evaluation

Four stages were used to define the state of proximity/adhesion of the two layers of the sinus mucosae, that is, elevated sinus mucosa (E-SM) and undetached sinus mucosa (U-SM). The stages included: No proximity, proximity, fusion, and synechia.

### 3.2 | No-proximity stage

The proximity stage was evaluated only in experiment E1 (Ferreira Balan et al., 2022), in which two periods of healing were studied at 2 and 10 weeks. In the sites without adhesions, in both periods of healing, the thinnest epithelial layer within 50  $\mu\text{m}$  from the MFR had smaller dimensions than those at the MFR and those at 100 and 200  $\mu\text{m}$  from the MFR. However, the epithelial layer at the MFR presented an increased dimension compared to the other layers during the 2-week period (Figure 3a) and decreased at the 10-week period (Figure 3b,c).

### 3.3 | Adhesion stages

The adhesion sites were evaluated in all included studies, that is, E1–E4.

In the “Proximity stage,” different periods of healing were included in the selected sites (Table 1), mostly at a 2-week period (17 cases), 5 at the 4-week, 2 at the 8-week period, and 7 at the 10-week period. An increased mean dimension of the pseudostratified columnar epithelium was observed at all sites evaluated in both U-SM and E-SM, possibly because of the mitotic activity. In the “Proximity stage,” adhesion of the two mucosae was mostly observed close to the MFR (Figure 4a). In the adhesion region, the cilia of the two epithelial layers were shortened and interlinked within the mucous context (Figure 4a,b). Hyperactivity of the goblet cells was also observed (Figure 4a,b). In other cases, the hyperplastic epithelium attempted to reach the opposite mucosa (Figure 4c,d).

The “Fusion stage” presented regions with epithelial cells of the two mucosae penetrating each other (Figure 5a). Epithelial cells of the two mucosae adhered. However, based on the available histology, it is difficult to define the boundaries between the two opposing layers. Bridges of epithelial cells connecting the two mucosae were also observed, delimiting enclosed regions within the sinus cavity, probably tubular in shape. These appeared as islands because of the two-dimensional appearance of the ground sections (Figure 5b,c). These structures might also be observed in the CBCTs (Figure 1a–d). Several hyperplastic projections were observed in both layers, located in opposite positions as if they were attracted to each other (Figure 5c). Some areas showed a loss of cells in the basal layer and appeared to be invaded by connective tissue and a few inflammatory cells (Figure 5a). Areas with a thin epithelial layer were also observed (Figures 5b and 6a).

In the “Synechia stage,” complete loss of the epithelium, with the formation of synechia represented by bridges of connective tissue and connecting the two lamina propria, was observed. The synechia exhibited fibroblast-like cells and fibers. No vessels or glands were observed, although their presence cannot be excluded (Figure 6a–c).

### 3.4 | Histological assessments

#### 3.4.1 | No-proximity stage

In an experiment (Ferreira Balan et al., 2022), 70 out of 80 mucosal folding regions (MFRs) were evaluated in 40 sinuses. Ten sites were excluded due to mucosal damage in the region of interest during biopsy or histological processing. The categorization resulted in 61 “No proximity” sites (90%), 4 “Proximity,” 4 “Fusion,” and 1 “Synechia” sites. The thinnest epithelial layer close to MFR (distance < 50  $\mu\text{m}$ ) was 15.2  $\mu\text{m}$  after 2 weeks and 13.1  $\mu\text{m}$  after 10 weeks (Table 2). The layer in the center of MFR measured 23.2 and 15.2  $\mu\text{m}$  after 2 and 10 weeks, respectively. In a few cases, the center of the MFR corresponded to the thinnest epithelial layer, particularly during the 10 weeks period. The evaluation of the “No-Proximity” sites

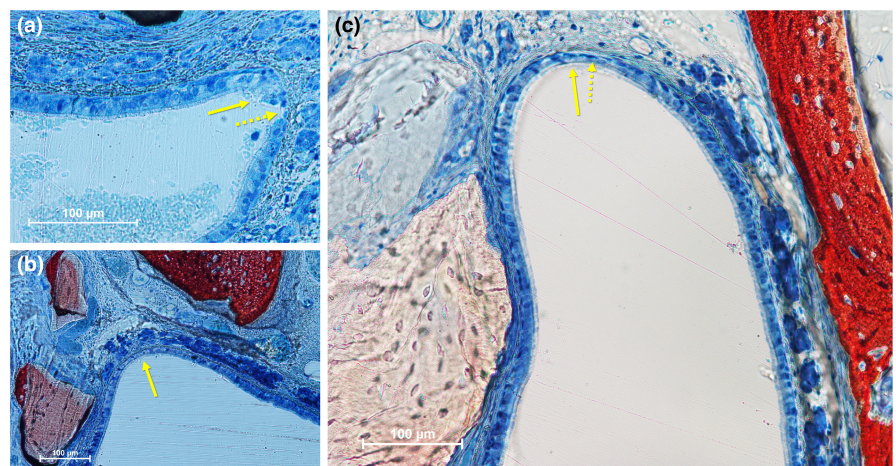


**FIGURE 3** Photomicrographs of ground sections representing MFR at no-proximity sites. (a) 2 weeks of healing; (b, c) 10 weeks of healing. Thinnest epithelial layer within 50  $\mu\text{m}$  from the MFR (dotted yellow arrows) and MFR center (yellow arrows). Stevenel's blue and alizarin red stain.

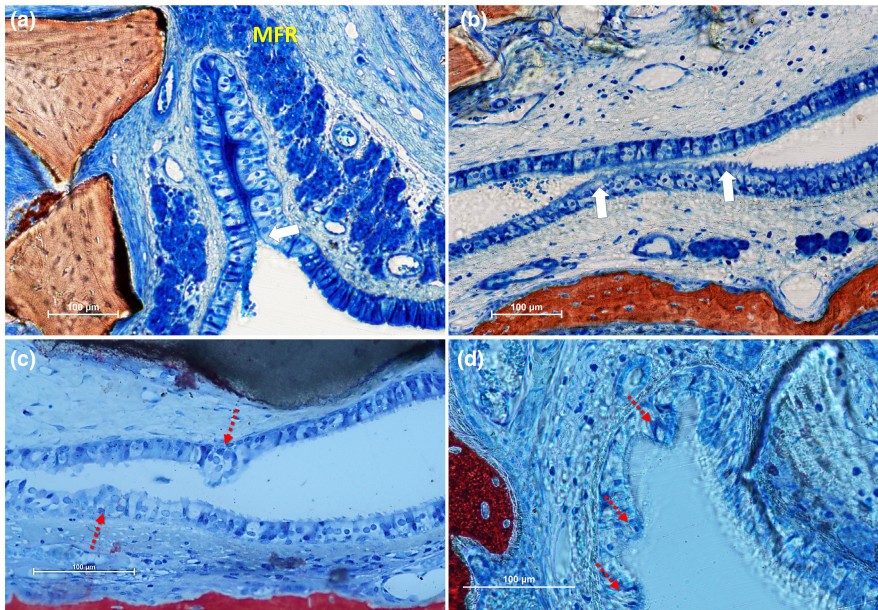


**FIGURE 4** Photomicrographs of ground sections representing the proximity stage after 2 weeks of healing. (a, b) Elevated and undetached sinus mucosae in contact with each other or in close vicinity with mucous interposed. The epithelium layers appeared to increase in dimension and to be in a hyperplastic stage. The white arrows indicate the limits of the adhesion subjectively determined. (c, d) The hyperplastic epithelium showed attempts to reach the opposite mucosa (dotted red arrows). Stevenel's blue and alizarin red stain.

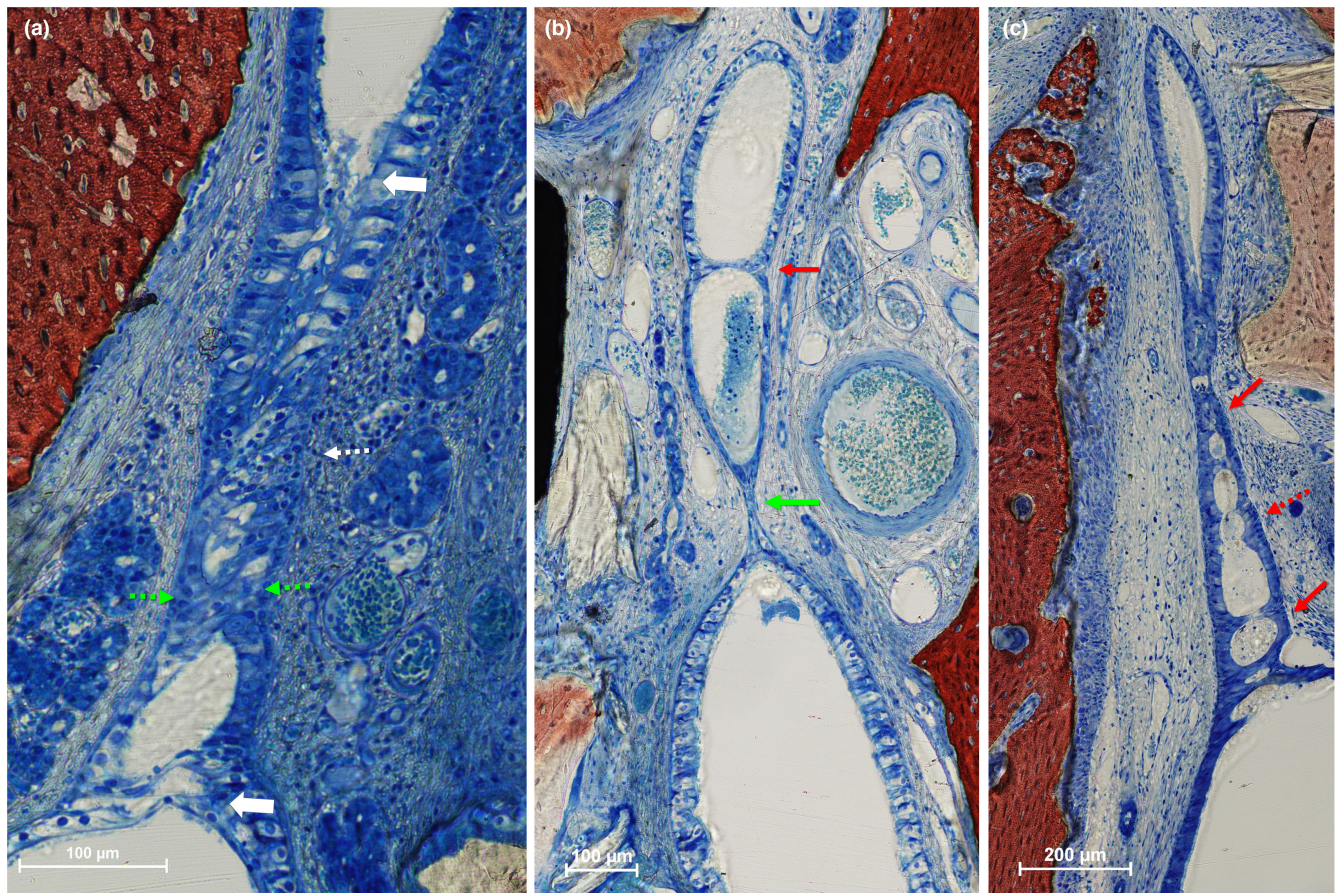


**FIGURE 5** Photomicrographs of ground sections representing the proximity stage after 2 weeks of healing. (a, b) Elevated and undetached sinus mucosae in contact with each other or in close vicinity with mucous interposed. The epithelium layers appeared increased in dimension and to be in a hyperplastic stage. The white arrows indicate the limits of the adhesion subjectively determined. (c, d) The hyperplastic epithelium showed attempts to reach the opposite mucosa (dotted red arrows). Stevenel's blue and alizarin red stain.

assessed at 100 and 200  $\mu\text{m}$  from the MFR provided a similar width of the epithelial layer for the elevated (range 17.6–19.1  $\mu\text{m}$ ) and undetached (16.8–18.9  $\mu\text{m}$ ) mucosae, which was found to be slightly

smaller in the 10-week than in the 2-week periods (Table 2). No statistically significant differences were found between U-SM and E-SM at any distance from the MFR. The differences between the

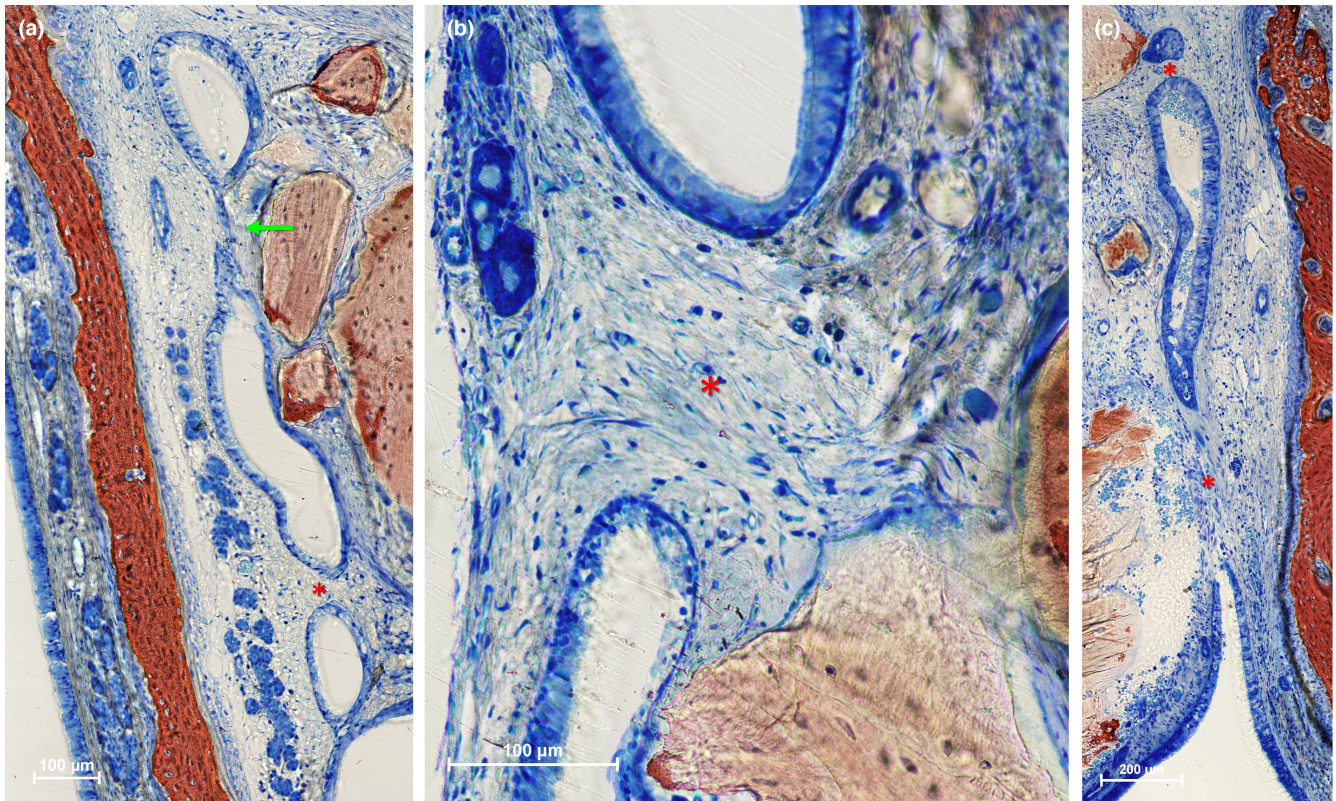


**FIGURE 6** Photomicrographs of ground sections representing the Synechia stage. Bridges of connective tissue connecting the two laminae propriae (red asterisks). Thin epithelial layer (green arrow). (a) Eight weeks of healing; (b, c) 2 weeks of healing. Stevenel's blue and alizarin red stain.

**TABLE 2** Epithelial layer width in the various sites evaluated in the no-proximity sites ( $n=61$ ) of Experiment E1.

	Thinnest layer	MFR	U-SM 100	U-SM 200	E-SM 100	E-SM 200	Distance 100	Distance 200
2 weeks	15.2±2.8	23.2±6.8	18.9±6.4	18.8±3.0	18.4±4.7	19.1±3.7	131.4±59.4	184.6±58.7
10 weeks	13.1±3.3	15.2±6.4	16.9±3.9	16.8±2.7	17.6±5.1	18.3±4.2	155.6±32.6	222.4±62.4

Note: No statistically significant differences were found between U-SM and E-SM at any distance from MFR. The difference between the thinnest layer and all other layers and between distances 100 and 200 were statistically significant. Only the difference between thinnest layer and center of the MFR in the 10 weeks period was not statistically significant. The measurements are expressed in micrometers.

Abbreviations: E-SM, elevated sinus mucosa; MFR, mucosa folding region; U-SM, undetached sinus mucosa.

thinnest layer and all other layers, and between distances of 100 and 200  $\mu\text{m}$ , were statistically significant. Only the difference between the thinnest layer and center of the MFR during the 10 weeks period was not statistically significant.

The distance between the undetached and elevated sinus mucosa measured at 100  $\mu\text{m}$  from the MFR was lower than that at 200  $\mu\text{m}$  and increased between 2 and 10 weeks at both distances.

### 3.4.2 | Adhesion stages

One hundred and fifty-two sinuses of seventy-six rabbits, with two MFRs per sinus (304 MFRs), were analyzed for adhesion site identification. Thirty-one (10%) sites presenting the adhesion phenomenon were found in the four experiments analyzed (Ferreira Balan et al., 2022; Godoy et al., 2021; Hirota et al., 2020; Masuda

et al., 2020) resulting in the following three categories: 12 sites were classified as "Proximity," 15 as "Fusion," and 4 as "Synechiae." The width of the epithelial layer evaluated at the adhesion sites was greater than that of the undetached pristine regions (Table 3). The P-SM was 19.5  $\mu\text{m}$ , whereas the thinnest layer close to the MFR was 19.3  $\mu\text{m}$ . At the center of the MFR, the epithelial width was 29.7  $\mu\text{m}$ . The epithelial layers in both U-SM and E-SM, as assessed at 100 and 200  $\mu\text{m}$  from the MFR, ranged from 23.8 to 27.0  $\mu\text{m}$ . The differences were statistically significant for all regions evaluated, with the exclusion of the thinnest layer and the elevated mucosa at 200  $\mu\text{m}$  from the MFR.

The distance between U-SM and E-SM measured at 100 and 200  $\mu\text{m}$  from MFR was 66.6 and 77.4  $\mu\text{m}$ , respectively.

The mucosal adhesions (Table 4) were found at a mean distance from MFR of 289.9  $\mu\text{m}$  (range 0–2135.8  $\mu\text{m}$ ). In 11 cases, the adhesion started from the MFR. The mean length of the adhesion was

168.8 $\mu$ m (range 7.2–551.8 $\mu$ m). The mean minimum distance between U-SM and E-SM was 1.4 $\mu$ m (range 0.0–12.2 $\mu$ m). The mean maximum epithelial width was 42.5 $\mu$ m (range 20.9–120.2 $\mu$ m). The differences between the maximum epithelial width and the width of the other regions were statistically significant.

## 4 | DISCUSSION

In the present study, healing occurred after maxillary sinus floor elevation when the elevated mucosa was in contact with the undetached mucosa still lying on the bony walls of the sinus.

In an experiment (Ferreira Balan et al., 2022), all sites were evaluated, and out of 80 mucosal folding regions (MFR), 70 could be analyzed, resulting in 61 “No proximity” sites, 4 “Proximity”, 4 “Fusion,” and 1 “Synechia” sites. The “No proximity” sites evaluated at 100 and 200 $\mu$ m from the MFR presented a mean width <20 $\mu$ m at all sites, without statistically significant differences. The only epithelial layer with a width >20 $\mu$ m (~23 $\mu$ m) was located at the MFR evaluated at 2 weeks. However, this layer decreased in size to <20 $\mu$ m during the 10-week period. The width of the epithelial layers slightly decreased during the 10-week period compared with the 2-week period at all sites examined. This might be interpreted as a mitotic stimulus of the epithelium, activation of goblet cells, and bleeding/edema subsequent to surgical procedures (Guo et al., 2016; Makary et al., 2016; Sakuma et al., 2020; Scala et al., 2012). This mitotic activity might have been prolonged to the 2-week period but decreased during the 10-week period. The distance between the undetached (U-SM) and elevated sinus mucosae (E-SM) was >130 $\mu$ m and >180 $\mu$ m, respectively, during the 2-week period. Both increased between 2 and 10 weeks, indicating shrinkage of the elevated space over time. Another characteristic of this stage of healing was the presence of the thinnest epithelial layers close to the MFR (<50 $\mu$ m). In only a few cases during the 10-week period did the thinnest layers coincide with the MFR.

Thirty-one adhesion phenomena were observed out of 304 sites examined in the four studies, presenting a frequency of approximately 10%. Twelve sites (4) were classified as “Proximity,” 15 (5) as “Fusion,” and 4 (1.3) as “Synechia.” The proximity between the two mucosae seems to have triggered these healing characteristics, which tend to fuse the two epithelia until they disintegrate, creating continuity between the lamina propria of the two layers. The increased width of the layers was due to increased epithelial mitotic and goblet cell activity. In some regions, this activity was more

pronounced, producing a large width of the epithelium, showing a tendency to grow toward the opposite layer.

The distance between the two layers in the adhesion stage was <80 $\mu$ m, which was two to three times lower than that of the “No Proximity stage,” as measured at 100 and 200 $\mu$ m from the MFR. Given that in the adhesion sites, an increased width of the epithelium was observed at 100 and 200 $\mu$ m from the MFR, it is suggested that the distance between the U-SM and E-SM might play a role in triggering hyperactivity and attraction between the two epithelial layers. The adhesion phenomenon was also observed when the two layers were not in direct contact, displaying crests projecting toward the opposite side and creating epithelial bridges connecting the two opposite layers. This attraction might be due to cell polarity or biochemical stimuli (Gómez et al., 2021; Jacinto et al., 2001; Pinto et al., 2019) which might act at a certain minimum distance. In the “fusion stage,” the two epithelia also showed interpenetrating properties similar to those described for bone and  $\beta$ -TCP/HA used for sinus elevation in rabbits (Tanaka et al., 2020). The epithelial cells of one layer were interconnected with those of the opposite layer, such as intertwined hand fingers, perhaps through desmosomal contacts. Finally, the epithelia were disrupted by the inflammatory cells (Figure 5a) or gradually disintegrated until they disappeared. Moreover, epithelial fusion has been described in wound closure (Martin & Suzanne, 2022), embryogenesis, neural tube closure, and palatal shell bridging (Jacinto et al., 2001; Mima et al., 2013).

The final stage was represented by bridging of the two layers of the lamina propria without an interposed epithelium, forming synechia that connected the lamina propria of the two opposing layers. The various stages of the adhesion phenomenon appeared to be a response of the sinus mucosa to the nonphysiological condition represented by the tight contact between the two layers, that is, U-SM and E-SM. This property of the sinus mucosae has also been reported in other studies in which attempts of the sinus mucosae to close perforations created by sharpened edges of granules of biomaterial used for sinus floor elevation have been shown (Miki et al., 2021).

As a consequence of surgery or infection, adhesions and synechia have also been observed in the eyes (Al-Hedaithy & Al-Kaff, 1993; Anitha et al., 2022; Do et al., 2016; Zhang et al., 2021), nose, which may have resulted in a reduction in airflow (Senanayake et al., 2021), and the uterus (Cho, 2017; Fouks et al., 2022; Lee et al., 2021; Rathat et al., 2011). Peritoneal adhesion and synechia formation are common characteristics of abdominal or pelvic surgery (Ha et al., 2016; Lang et al., 2010; Sun et al., 2020). They may trigger complications such as intestinal or small-bowel obstructions,

TABLE 3 Epithelial layer width in pristine and adhesion regions.

P-SM	Thinnest layer	MFR	U-SM 100	U-SM 200	E-SM 100	E-SM 200	Distance 100	Distance 200
19.5 $\pm$ 6.4	19.3 $\pm$ 10.0	29.7 $\pm$ 12.9	25.5 $\pm$ 12.6	24.1 $\pm$ 13.4	27.0 $\pm$ 16.5	23.8 $\pm$ 14.4	66.6 $\pm$ 48.0	77.4 $\pm$ 65.0

Note: The differences between the pristine and adhesion regions' epithelium width were statistically significant with the exception of the thinnest layer and the elevated mucosa at 200 $\mu$ m from MFR.

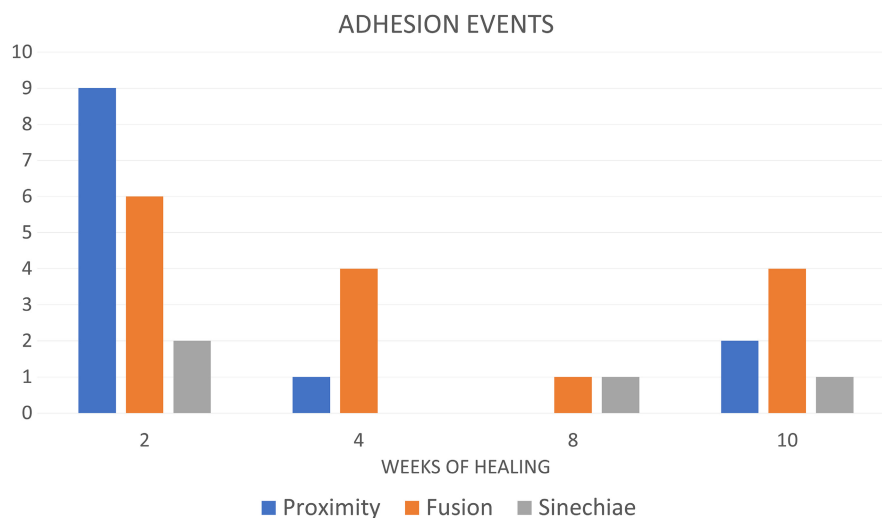


**TABLE 4** Linear measurements in micrometers in the adhesion regions.

	Distance from MFR	Length of adhesion	Min distance U-SM and E-SM	Max layer width
Mean ± SD	289.9 ± 432.7	168.8 ± 123.2	1.4 ± 3.1	42.5 ± 19.6
Min	0.0	7.2	0.0	20.9
Max	2135.8	551.8	12.2	120.2

Note: The differences between maximum epithelial width and width of the other regions were statistically significant.

**FIGURE 7** Number of adhesion events per period examined.



infertility, and chronic abdominal and pelvic pain (Chegini, 2008; Liakakos et al., 2001; Makama et al., 2017). Synechiae are generally referred to as “scar tissue.” However, biopsies collected from peritoneal adhesions present arterioles, venules, capillaries, and myelinated and nonmyelinated nerve fibers (Herrick et al., 2000; Sulaiman et al., 2000). In the present study, the few ground sections presenting synechiae did not allow the observation of the structures mentioned.

Adhesion phenomena and synechiae in the sinus might occur after the removal of antrochoanal polyps (Al-Balas et al., 2020; Kelles et al., 2014) and the surgical treatment of chronic sinusitis (Kende et al., 2019; McCoul et al., 2012) or oro-antral fistula (Horowitz et al., 2016) and have been described as common minor and underreported complications after sinus surgery (Bhatki & Goldberg, 2009). Depending on the location, the synechiae may remain asymptomatic or create obstruction if they are located close to the ostium of the sinus cavity. These phenomena were also observed in the experiments included in the present study. The contact of two layers of epithelium, such as the peritoneum, pleura, gastrointestinal tract, or oral mucosa, is a normal condition in the human body. However, inflammatory reactions due to infections or surgery may create conditions for the formation of adhesions. Detachment from the bone wall of the elevated mucosa and the consequent edema that may reach the ostium might trigger the adhesion phenomenon between the elevated and undetached mucosae when they are in close contact.

In the present study, adhesions and synechiae formed enclosed regions with probable tubular shapes. It may be argued that

mucous produced by mucous glands and goblet cells might drain toward the sinus cavity. However, if the two ends are closed, the secluded space may lead to cyst formation or trigger infection and sinusitis. Sinusitis is a well-described complication that might occur after sinus floor elevation (Hsu et al., 2022), and the formation of these secluded spaces should be considered as possible reason for sinusitis, together with mucosal perforation and biomaterial extrusion within the sinus cavity (Doud Galli et al., 2001; Testori et al., 2020; Urban et al., 2012). The experiments included in the present article were initially meant for other purposes, and the adhesion phenomenon was discovered during histological evaluation. To our knowledge, no data have been reported on adhesion phenomena after maxillary sinus floor elevation; therefore, we believe that it is important that the scientific community and clinicians are aware of this phenomenon. These data might allow future studies at the cellular and molecular levels.

In the two-dimension histological evaluation used in the present study, only 10% of the occurrences were detected. The presence of adhesion sites in humans after sinus floor elevation has not yet been evaluated, but may still occur (Figure 1a–d). Currently, we can only speculate on possible complications. Future analyses in humans might reveal that no complications are associated with the presence of close contact between the two mucosal layers. Moreover, even though radiographic assessment might reveal contact between the two mucosal layers, the presence of a true adhesion phenomenon cannot be inferred. However, we can suggest taking into account the phenomenon of adhesion and following patients for possible complications after sinus floor elevation. Medico-legal issues should not

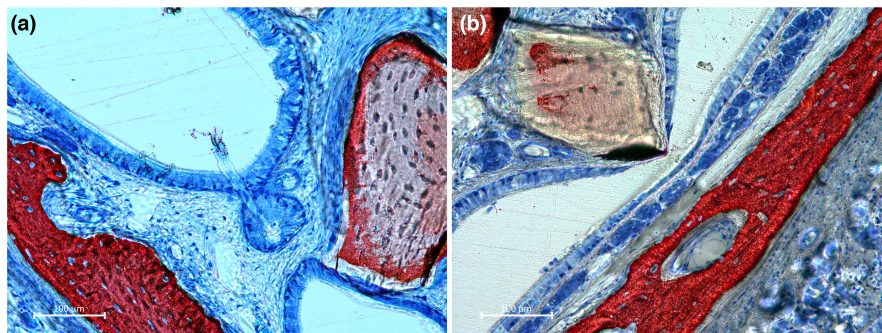


**FIGURE 8** A close contact with the sinus mucosa of granules of biomaterial may interfere with the adhesion phenomena as damages to the sinus mucosa may occur. (a) No sign of damages; (b) thinning of both elevated and undetached mucosae and perforation of the elevated mucosa.

be excluded if complications arise or if symptoms are referred by the patients in the presence of adhesions (Figure 1a–d).

In the present study, all adhesion stages were more represented in the 2 weeks period, as documented by the higher number of samples evaluated (Figure 7). Adhesion sites were still present during the 10 weeks period. Even though the number of sites presenting adhesion is too low to allow a strong interpretation, it is suggested that the stage of “proximity” should be a reversible situation that may allow the restoration of the two layers of the sinus mucosa. However, the “fusion-” and “synechia stages” may be irreversible.

The main limitation of the present study is related to the model used, which presents a thinner sinus mucosa (Aimetti et al., 2008; Iida et al., 2017; Janner et al., 2011) and a faster rate of healing (Botticelli & Lang, 2017) than in humans. Adhesions were not a frequent finding in the large material evaluated (approximately 10%), and the synechiae were too few to allow for proper analysis. The results of the present study allowed the description of some healing characteristics of adhesion between undetached and elevated sinus mucosae. However, the cellular and molecular mechanisms underlying this phenomenon require further investigation. Synechiae were detected after 2 weeks. During this period, several fusion stages were also observed. Progression of later conditions toward a more advanced stage cannot be excluded. An analysis of longer healing periods should be included. Moreover, it should be taken into consideration that close contact with the sinus mucosa of granules of biomaterial may interfere with the adhesion phenomena as damage to the sinus mucosa may occur. (Figure 8a,b; Kato et al., 2021; Miki et al., 2021).

In conclusion, close proximity or contact between the elevated and undetached mucosae still adhered to the bony walls occasionally observed after maxillary sinus floor elevation may encompass hyperplasia of the epithelial cells and adhesion of the two layers of the sinus mucosae, eventually resulting in synechiae. However, the clinical implications of these adhesion phenomena remain unknown and require further exploration.

#### AUTHOR CONTRIBUTIONS

DB and YN conceived the ideas. KAAA and EFDR collected the data. DB and EFDR analyzed the data. DB, YN, and NPL led the writing. SPX supervised the investigation and provided the resources. All authors have read and approved the final manuscript.

#### ACKNOWLEDGMENTS

We acknowledge the contribution of Sebastião Bianco (Faculty of Dentistry of Ribeirão Preto, SP, Brazil) for histological processing. The Cerabone® xenograft was provided free of charge by Straumann Italy, Milan, Italy.

#### FUNDING INFORMATION

The study was funded by ARDEC Academy, Rimini, Italy.

#### CONFLICT OF INTEREST STATEMENT

The authors declare no conflicts of interest.

#### DATA AVAILABILITY STATEMENT

The data that support the findings of this study are available from the corresponding author upon reasonable request.

#### ORCID

Karol Alí Apaza Alccayhuaman  <https://orcid.org/0000-0003-4565-5222>

[org/0000-0003-4565-5222](https://orcid.org/0000-0003-4565-5222)

Daniele Botticelli  <https://orcid.org/0000-0003-2804-1632>

Niklaus Peter Lang  <https://orcid.org/0000-0002-6938-9611>

Samuel Porfirio Xavier  <https://orcid.org/0000-0001-7389-5886>

#### REFERENCES

- Aimetti, M., Massei, G., Morra, M., Cardesi, E., & Romano, F. (2008). Correlation between gingival phenotype and Schneiderian membrane thickness. *The International Journal of Oral & Maxillofacial Implants*, 23(6), 1128–1132.
- Al-Balas, H. I., Farneti, P., Bellusci, A., Crocetta, F. M., Sollini, G., & Pasquini, E. (2020). A comparison of two endoscopic techniques for the treatment of antrochoanal polyps. *Acta Otorhinolaryngologica Italica*, 40(4), 290–296. <https://doi.org/10.14639/0392-100x-n0259>
- Al-Hedaithy, S. S., & Al-Kaff, A. S. (1993). Exophiala jeanselmei keratitis. *Mycoses*, 36(3–4), 97–100. <https://doi.org/10.1111/j.1439-0507.1993.tb00695.x>
- Anitha, V., Ravindran, M., Jacob, A. D., Ghorpade, A., & Uduman, M. S. (2022). Outcomes of optical penetrating keratoplasty with the large sized donor for failed therapeutic grafts for infectious keratitis from the tertiary eye care center, South India. *European Journal of Ophthalmology*, 32(6), 3411–3419. <https://doi.org/10.1177/112067212211086143>
- Bhatki, A. M., & Goldberg, A. N. (2009). CHAPTER 42 – Complications of surgery of the paranasal sinuses. In D. W. Eisele & R. V. Smith (Eds.), *Complications in head and neck surgery* (2nd ed., pp. 543–558). Mosby.
- Botticelli, D., & Lang, N. P. (2017). Dynamics of osseointegration in various human and animal models – A comparative analysis. *Clinical*

- Oral Implants Research*, 28(6), 742–748. <https://doi.org/10.1111/clr.12872>
- Chegini, N. (2008). TGF-beta system: The principal profibrotic mediator of peritoneal adhesion formation. *Seminars in Reproductive Medicine*, 26(4), 298–312. <https://doi.org/10.1055/s-0028-1082388>
- Cho, H. J. (2017). An intrauterine fetal death due to horizontal uterine synechia. *Taiwanese Journal of Obstetrics & Gynecology*, 56(3), 406–407. <https://doi.org/10.1016/j.tjog.2016.12.009>
- Del Fabbro, M., Wallace, S. S., & Testori, T. (2013). Long-term implant survival in the grafted maxillary sinus: A systematic review. *The International Journal of Periodontics & Restorative Dentistry*, 33(6), 773–783. <https://doi.org/10.11607/prd.1288>
- Do, J. R., Lee, H., Baek, S., Lee, T. S., & Chang, M. (2016). Efficacy of postoperative mitomycin-C eye drops on the clinical outcome in endoscopic dacryocystorhinostomy. *Graefe's Archive for Clinical and Experimental Ophthalmology*, 254(4), 785–790. <https://doi.org/10.1007/s00417-015-3229-2>
- Doud Galli, S. K., Lebowitz, R. A., Giacchi, R. J., Glickman, R., & Jacobs, J. B. (2001). Chronic sinusitis complicating sinus lift surgery. *American Journal of Rhinology*, 15(3), 181–186. <https://doi.org/10.2500/105065801779954120>
- Ferreira Balan, V., Botticelli, D., Peñarrocha-Oltra, D., Masuda, K., Pires Godoy, E., & Xavier, S. P. (2022). Maxillary sinus floor augmentation with two different inorganic bovine bone grafts: An experimental study in rabbits. *The Chinese Journal of Dental Research*, 25(2), 93–105. <https://doi.org/10.3290/j.cjdr.b3086337>
- Figueiredo, M., Henriques, J., Martins, G., Guerra, F., Judas, F., & Figueiredo, H. (2010). Physicochemical characterization of biomaterials commonly used in dentistry as bone substitutes – Comparison with human bone. *Journal of Biomedical Materials Research. Part B, Applied Biomaterials*, 92(2), 409–419. <https://doi.org/10.1002/jbm.b.31529>
- Fouks, Y., Kidron, A., Lavie, I., Shapira, Z., Cohen, Y., Levin, I., Azem, F., & Cohen, A. (2022). Reproductive outcomes and overall prognosis of women with Asherman's syndrome undergoing IVF. *Journal of Minimally Invasive Gynecology*, 29(11), 1253–1259. <https://doi.org/10.1016/j.jmig.2022.08.004>
- Godoy, E. P., Alccayhuaman, K. A. A., Botticelli, D., Amaroli, A., Balan, V. F., Silva, E. R., & Xavier, S. P. (2021). Osteoconductivity of bovine xenograft granules of different sizes in sinus lift: A histomorphometric study in rabbits. *Dentistry Journal*, 9(6), 61. <https://doi.org/10.3390/dj9060061>
- Gómez, H. F., Dumond, M. S., Hodel, L., Vetter, R., & Iber, D. (2021). 3D cell neighbour dynamics in growing pseudostratified epithelia. *eLife*, 10, e68135. <https://doi.org/10.7554/eLife.68135>
- Griffa, A., Berrone, M., Boffano, P., Viterbo, S., & Berrone, S. (2010). Mucociliary function during maxillary sinus floor elevation. *The Journal of Craniofacial Surgery*, 21(5), 1500–1502. <https://doi.org/10.1097/SCS.0b013e3181ef2be9>
- Guo, Z. Z., Liu, Y., Qin, L., Song, Y. L., Xie, C., & Li, D. H. (2016). Longitudinal response of membrane thickness and ostium patency following sinus floor elevation: A prospective cohort study. *Clinical Oral Implants Research*, 27(6), 724–729. <https://doi.org/10.1111/clr.12655>
- Ha, U. S., Koh, J. S., Cho, K. J., Yoon, B. I., Lee, K. W., Hong, S. H., & Lee, J. Y. (2016). Hyaluronic acid-carboxymethylcellulose reduced postoperative bowel adhesions following laparoscopic urologic pelvic surgery: A prospective, randomized, controlled, single-blind study. *BMC Urology*, 16(1), 28. <https://doi.org/10.1186/s12894-016-0149-3>
- Herrick, S. E., Mutsaers, S. E., Ozua, P., Sulaiman, H., Omer, A., Boulos, P., Foster, M. L., & Laurent, G. J. (2000). Human peritoneal adhesions are highly cellular, innervated, and vascularized. *The Journal of Pathology*, 192(1), 67–72. [https://doi.org/10.1002/1096-9896\(2000\)999:9999::Aid-path678>3.0.Co;2-e](https://doi.org/10.1002/1096-9896(2000)999:9999::Aid-path678>3.0.Co;2-e)
- Hirota, A., Yamada, Y., Canullo, L., Xavier, S. P., & Baba, S. (2020). Bioactivation of bovine bone matrix using argon plasma: An experimental study for sinus augmentation in rabbits. *The International Journal of Oral & Maxillofacial Implants*, 35(4), 731–738. <https://doi.org/10.11607/jomi.8385>
- Horowitz, G., Koren, I., Carmel, N. N., Balaban, S., Abu-Ghanem, S., Fliss, D. M., Kleinman, S., & Reiser, V. (2016). One stage combined endoscopic and per-oral buccal fat pad approach for large oro-antral-fistula closure with secondary chronic maxillary sinusitis. *European Archives of Oto-Rhino-Laryngology*, 273(4), 905–909. <https://doi.org/10.1007/s00405-015-3656-z>
- Hsu, Y. T., Rosen, P. S., Choksi, K., Shih, M. C., Ninneman, S., & Lee, C. T. (2022). Complications of sinus floor elevation procedure and management strategies: A systematic review. *Clinical Implant Dentistry and Related Research*, 24(6), 740–765. <https://doi.org/10.1111/cid.13086>
- Iida, T., Carneiro Martins Neto, E., Botticelli, D., Apaza Alccayhuaman, K. A., Lang, N. P., & Xavier, S. P. (2017). Influence of a collagen membrane positioned subjacent the sinus mucosa following the elevation of the maxillary sinus. A histomorphometric study in rabbits. *Clinical Oral Implants Research*, 28(12), 1567–1576. <https://doi.org/10.1111/clr.13027>
- Jacinto, A., Martinez-Arias, A., & Martin, P. (2001). Mechanisms of epithelial fusion and repair. *Nature Cell Biology*, 3(5), E117–E123. <https://doi.org/10.1038/35074643>
- Janner, S. F., Caversaccio, M. D., Dubach, P., Sendi, P., Buser, D., & Bornstein, M. M. (2011). Characteristics and dimensions of the Schneiderian membrane: A radiographic analysis using cone beam computed tomography in patients referred for dental implant surgery in the posterior maxilla. *Clinical Oral Implants Research*, 22(12), 1446–1453. <https://doi.org/10.1111/j.1600-0501.2010.02140.x>
- Kato, S., Botticelli, D., De Santis, E., Kanayama, M., Ferreira, S., & Rangel-Garcia, I., Jr. (2021). Sinus mucosa thinning and perforation after sinus augmentation: A histological study in rabbits. *Oral and Maxillofacial Surgery*, 25(4), 477–485. <https://doi.org/10.1007/s10006-021-00946-y>
- Kawakami, S., Botticelli, D., Nakajima, Y., Sakuma, S., & Baba, S. (2019). Anatomical analyses for maxillary sinus floor augmentation with a lateral approach: A cone beam computed tomography study. *Annals of Anatomy*, 226, 29–34. <https://doi.org/10.1016/j.aanat.2019.07.003>
- Kawakami, S., Lang, N. P., Ferri, M., Apaza Alccayhuaman, K. A., & Botticelli, D. (2019). Influence of the height of the antrostomy in sinus floor elevation assessed by cone beam computed tomography – A randomized clinical trial. *The International Journal of Oral & Maxillofacial Implants*, 34(1), 223–232. <https://doi.org/10.11607/jomi.7112>
- Kawakami, S., Lang, N. P., Iida, T., Ferri, M., Apaza Alccayhuaman, K. A., & Botticelli, D. (2018). Influence of the position of the antrostomy in sinus floor elevation assessed with cone-beam computed tomography: A randomized clinical trial. *Journal of Investigative and Clinical Dentistry*, 9(4), e12362. <https://doi.org/10.1111/jicd.12362>
- Kelles, M., Toplu, Y., Yildirim, I., & Okur, E. (2014). Antrochoanal polyp: Clinical presentation and retrospective comparison of endoscopic sinus surgery and endoscopic sinus surgery plus mini-Caldwell surgical procedures. *The Journal of Craniofacial Surgery*, 25(5), 1779–1781. <https://doi.org/10.1097/scs.0000000000000901>
- Kende, P., Mathai, P. C., Landge, J., Aggarwal, N., Ghodke, M., Chellappa, N., & Meshram, V. (2019). Combined endoscopic and intra-oral approach for chronic maxillary sinusitis of dental origin—a prospective clinical study. *Oral and Maxillofacial Surgery*, 23(4), 429–437. <https://doi.org/10.1007/s10006-019-00792-z>
- Lang, R., Baumann, P., Jauch, K. W., Schmoor, C., Weis, C., Odermatt, E., & Knaebel, H. P. (2010). A prospective, randomised, controlled, double-blind phase I-II clinical trial on the safety of A-part gel as adhesion prophylaxis after major abdominal surgery versus non-treated group. *BMC Surgery*, 10, 20. <https://doi.org/10.1186/1471-2482-10-20>

- Lee, W. L., Liu, C. H., Cheng, M., Chang, W. H., Liu, W. M., & Wang, P. H. (2021). Focus on the primary prevention of intrauterine adhesions: Current concept and vision. *International Journal of Molecular Sciences*, 22(10), 5175. <https://doi.org/10.3390/ijms22105175>
- Liakakos, T., Thomakos, N., Fine, P. M., Dervenis, C., & Young, R. L. (2001). Peritoneal adhesions: Etiology, pathophysiology, and clinical significance. Recent advances in prevention and management. *Digestive Surgery*, 18(4), 260–273. <https://doi.org/10.1159/000050149>
- Makama, J. G., Kache, S. A., Ajah, L. J., & Ameh, E. A. (2017). Intestinal obstruction caused by appendicitis: A systematic review. *Journal of the West African College of Surgeons*, 7(3), 94–115.
- Makary, C., Rebaudi, A., Menhall, A., & Naaman, N. (2016). Changes in sinus membrane thickness after lateral sinus floor elevation: A radiographic study. *The International Journal of Oral & Maxillofacial Implants*, 31(2), 331–337. <https://doi.org/10.11607/jomi.4108>
- Martin, E., & Suzanne, M. (2022). Functions of Arp2/3 complex in the dynamics of epithelial tissues. *Frontiers in Cell and Development Biology*, 10, 886288. <https://doi.org/10.3389/fcell.2022.886288>
- Masuda, K., Silva, E. R., Apaza Alccayhuaman, K. A., Botticelli, D., & Xavier, S. P. (2020). Histologic and micro-CT analyses at implants placed immediately after maxillary sinus elevation using large or small xenograft granules: An experimental study in rabbits. *The International Journal of Oral & Maxillofacial Implants*, 35(4), 739–748. <https://doi.org/10.11607/jomi.8067>
- McCoul, E. D., Smith, T. L., Mace, J. C., Anand, V. K., Senior, B. A., Hwang, P. H., Stankiewicz, J. A., & Tabae, A. (2012). Interrater agreement of nasal endoscopy in patients with a prior history of endoscopic sinus surgery. *International Forum of Allergy & Rhinology*, 2(6), 453–459. <https://doi.org/10.1002/alar.21058>
- Miki, M., Botticelli, D., Silva, E. R., Xavier, S. P., & Baba, S. (2021). Incidence of sinus mucosa perforations during healing after sinus elevation using Deproteinized bovine bone mineral as grafting material: A histologic evaluation in a rabbit model. *The International Journal of Oral & Maxillofacial Implants*, 36(4), 660–668. <https://doi.org/10.11607/jomi.8580>
- Mima, J., Koshino, A., Oka, K., Uchida, H., Hieda, Y., Nohara, K., Kogo, M., Chai, Y., & Sakai, T. (2013). Regulation of the epithelial adhesion molecule CEACAM1 is important for palate formation. *PLoS One*, 8(4), e61653. <https://doi.org/10.1371/journal.pone.0061653>
- Pinto, C. S., Khandekar, A., Bhavna, R., Kiesel, P., Pigino, G., & Sonawane, M. (2019). Microridges are apical epithelial projections formed of F-actin networks that organize the glycan layer. *Scientific Reports*, 9(1), 12191. <https://doi.org/10.1038/s41598-019-48400-0>
- Pjetursson, B. E., Tan, W. C., Zwahlen, M., & Lang, N. P. (2008). A systematic review of the success of sinus floor elevation and survival of implants inserted in combination with sinus floor elevation. *Journal of Clinical Periodontology*, 35(8 Suppl), 216–240. <https://doi.org/10.1111/j.1600-051X.2008.01272.x>
- Rathat, G., Do Trinh, P., Mercier, G., Reyftmann, L., Dechanet, C., Boulot, P., & Giacalone, P. L. (2011). Synechia after uterine compression sutures. *Fertility and Sterility*, 95(1), 405–409. <https://doi.org/10.1016/j.fertnstert.2010.08.055>
- Sakuma, S., Ferri, M., Imai, H., Fortich Mesa, N., Blanco Victorio, D. J., Apaza Alccayhuaman, K. A., & Botticelli, D. (2020). Involvement of the maxillary sinus ostium (MSO) in the edematous processes after sinus floor augmentation: A cone-beam computed tomographic study. *International Journal of Implant Dentistry*, 6(1), 35. <https://doi.org/10.1186/s40729-020-00233-7>
- Scala, A., Botticelli, D., Faeda, R. S., Garcia Rangel, I., Américo de Oliveira, J., & Lang, N. P. (2012). Lack of influence of the Schneiderian membrane in forming new bone apical to implants simultaneously installed with sinus floor elevation: An experimental study in monkeys. *Clinical Oral Implants Research*, 23(2), 175–181. <https://doi.org/10.1111/j.1600-0501.2011.02227.x>
- Senanayake, P., Salati, H., Wong, E., Bradshaw, K., Shang, Y., Singh, N., & Inthavong, K. (2021). The impact of nasal adhesions on airflow and mucosal cooling – A computational fluid dynamics analysis. *Respiratory Physiology & Neurobiology*, 293, 103719. <https://doi.org/10.1016/j.resp.2021.103719>
- Sulaiman, H., Gabella, G., Davis, C., Mutsaers, S. E., Boulos, P., Laurent, G. J., & Herrick, S. E. (2000). Growth of nerve fibres into murine peritoneal adhesions. *The Journal of Pathology*, 192(3), 396–403. [https://doi.org/10.1002/1096-9896\(2000\)999:999<::Aid-path710>3.0.Co;2-4](https://doi.org/10.1002/1096-9896(2000)999:999<::Aid-path710>3.0.Co;2-4)
- Sun, M. L., Zhang, Y., Wang, B., Ma, T. A., Jiang, H., Hu, S. L., Zhang, P., & Tuo, Y. H. (2020). Randomized controlled trials for comparison of laparoscopic versus conventional open catheter placement in peritoneal dialysis patients: A meta-analysis. *BMC Nephrology*, 21(1), 60. <https://doi.org/10.1186/s12882-020-01724-w>
- Tan, W. C., Lang, N. P., Zwahlen, M., & Pjetursson, B. E. (2008). A systematic review of the success of sinus floor elevation and survival of implants inserted in combination with sinus floor elevation. Part II: Transalveolar technique. *Journal of Clinical Periodontology*, 35(8 Suppl), 241–254. <https://doi.org/10.1111/j.1600-051X.2008.01273.x>
- Tanaka, K., Botticelli, D., Canullo, L., Baba, S., & Xavier, S. P. (2020). New bone ingrowth into  $\beta$ -TCP/HA graft activated with argon plasma: A histomorphometric study on sinus lifting in rabbits. *International Journal of Implant Dentistry*, 6(1), 36. <https://doi.org/10.1186/s40729-020-00236-4>
- Testori, T., Yu, S. H., Tavelli, L., & Wang, H. L. (2020). Perforation risk assessment in maxillary sinus augmentation with lateral wall technique. *The International Journal of Periodontics & Restorative Dentistry*, 40(3), 373–380. <https://doi.org/10.11607/prd.4179>
- Torretta, S., Mantovani, M., & Pignataro, L. (2012). In reply to "mucociliary function during maxillary sinus floor elevation". *The Journal of Craniofacial Surgery*, 23(1), 346. <https://doi.org/10.1097/SCS.0b013e318242051c>
- Urban, I. A., Nagursky, H., Church, C., & Lozada, J. L. (2012). Incidence, diagnosis, and treatment of sinus graft infection after sinus floor elevation: A clinical study. *The International Journal of Oral & Maxillofacial Implants*, 27(2), 449–457.
- Zhang, M., Mao, G. Y., Ye, C., Fan, S. J., Liang, Y. B., & Wang, N. L. (2021). Association of peripheral anterior synechia, intraocular pressure, and glaucomatous optic neuropathy in primary angle-closure diseases. *International Journal of Ophthalmology*, 14(10), 1533–1538. <https://doi.org/10.18240/ijo.2021.10.09>

**How to cite this article:** Nakajima, Y., Apaza Alccayhuaman, K. A., Botticelli, D., Lang, N. P., De Rossi, E. F., & Xavier, S. P. (2023). Mucosal adhesion phenomenon after maxillary sinus floor elevation: A preclinical study. *Clinical Oral Implants Research*, 00, 1–12. <https://doi.org/10.1111/clr.14123>